

Dynamical Magnetic Susceptibilities in Cu Benzoate

Fabian H.L. Essler and Alexei M. Tsvelik

Department of Physics, Theoretical Physics, Oxford University
1 Keble Road, Oxford OX1 3NP, United Kingdom

Recent experiments on the quasi 1-D antiferromagnet Cu Benzoate revealed a magnetic field induced gap coexisting with (ferro)magnetic order. The theory explaining these findings has been put forward by Oshikawa and Affleck. In the present work we discuss consequences of this theory for inelastic neutron scattering experiments by calculating the dynamical magnetic susceptibilities close to the antiferromagnetic wave vector by the formfactor method.

PACS: 74.65.+n, 75.10. Jm, 75.25.+z

I. INTRODUCTION

It has been known for some time that Cu Benzoate is a quasi-1D $S = 1/2$ (Heisenberg) antiferromagnet [2]. In a recent neutron scattering experiment [1] in a magnetic field, the existence of field-dependent incommensurate low energy modes was established. The incommensurability was found to be consistent with the one predicted by the exact solution of the Heisenberg model in a magnetic field. However, the system exhibited an unexpected excitation gap induced by the applied field. These findings were quite surprising as the coexistence of a gap and a magnetization is inconsistent with rotational symmetry around the direction of the magnetization. This puzzle was resolved by Oshikawa and Affleck [3] who showed that a staggered magnetic field is generated *perpendicular* to the direction of the applied magnetic field. They proposed that Cu Benzoate is described by the Hamiltonian

$$H = \sum_i J \vec{S}_i \cdot \vec{S}_{i+1} - H S_i^x + h(-1)^i S_i^z, \quad (1)$$

where $H \gg h$. The low energy effective theory of (1) is obtained by abelian bosonization and is given by a Sine-Gordon model with Lagrangian density [3]

$$\mathcal{L} = \frac{1}{2}(\partial_\mu \phi)^2 + \lambda \cos(\beta \theta). \quad (2)$$

Here θ is the dual field and fulfils $\partial_x \phi = -\partial_t \theta$, $\partial_t \phi = -\partial_x \theta$. This implies that $(\partial_\mu \phi)^2 = (\partial_\mu \theta)^2$ and (2) thus is a Sine-Gordon model for the dual field.

The coupling constant β is a function of the applied field H and is related to the “dressed charge” (see [4] and references therein) of the isotropic Heisenberg chain in a magnetic field by

$$\beta = \frac{\sqrt{\pi}}{Z}. \quad (3)$$

For further convenience we define the quantity

$$\xi = \frac{\beta^2}{8\pi - \beta^2}. \quad (4)$$

The dressed charge can be determined exactly from the Bethe Ansatz solution. It is given by $Z = Z(A)$, where $Z(\lambda)$ is a solution of the integral equation [4]

$$Z(\lambda) + \frac{1}{2\pi} \int_{-A}^A d\mu \frac{2}{1 + (\lambda - \mu)^2} Z(\mu) = 1. \quad (5)$$

The integration boundary A is a function of the magnetic field H and is determined by the condition $\varepsilon(A) = 0$, where

$$\varepsilon(\lambda) + \frac{1}{2\pi} \int_{-A}^A d\mu \frac{2}{1 + (\lambda - \mu)^2} \varepsilon(\mu) = \frac{2H}{J} - \frac{2}{\lambda^2 + \frac{1}{4}}. \quad (6)$$

These integral equations can easily be solved numerically. In Fig. 1 we plot $\beta^2/2\pi$ of (where β is the coupling constant of the Sine-Gordon model (2)) as a function of the applied magnetic field H for Cu Benzoate. We note that at zero field $\beta^2/2\pi = 1$.

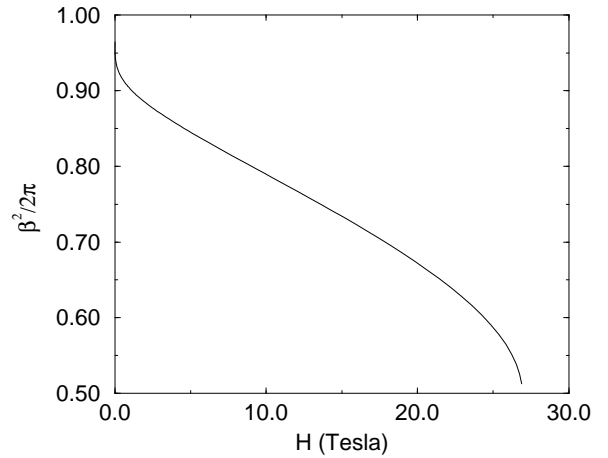


FIG. 1. Coupling constant $\beta^2/2\pi$ as a function of the applied magnetic field.

The curve in Fig. 1 terminates at a value of $H \approx 27$ Tesla ($H = 2J$) at which the underlying Heisenberg model experiences a transition to the saturated ferromagnetic state.

The spectrum of the Sine-Gordon theory (2) is well known [5] (see also [6,7]): it consists of a soliton-antisoliton doublet of mass M and their bound states which are called “breathers”. For Cu Benzoate the soliton mass as a function of the applied magnetic field was determined by Oshikawa and Affleck [3]

$$M \approx 1.85 \left(\frac{h}{J}\right)^{1/(2-\beta^2/4\pi)} J, \quad (7)$$

where the induced staggered field h is determined as a function of the applied field H (and the Dzyaloshinskii-Moriya interaction in Cu Benzoate) in [3].

In addition there are $[\frac{1}{\xi}]$ (here $[x]$ denotes the largest integer smaller than x) breathers, denoted by B_1, B_2, \dots , with masses

$$M_n = 2M \sin n\pi\xi/2; \quad n = 1, \dots, [1/\xi]. \quad (8)$$

The mass spectrum as a function of magnetic field for CuBenzoate is plotted in Fig. 2

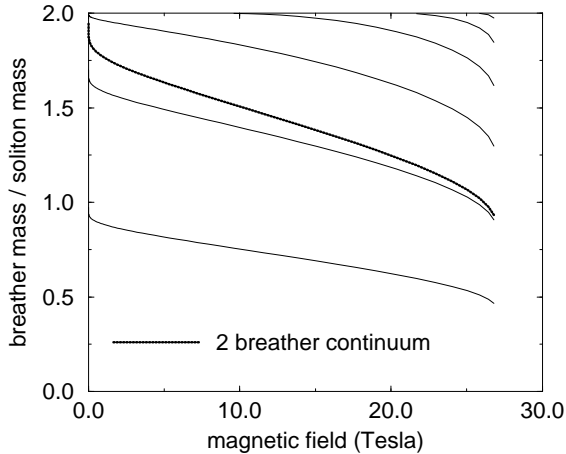


FIG. 2. Breather masses in units of the soliton mass as functions of the applied magnetic field.

We see that for small fields there are *three* breathers, one of which is just below the soliton-antisoliton continuum starting at $2M$. For higher fields further breathers split off this continuum. However they appear at energies higher than the threshold of the B_1B_1 two breather continuum. For small fields the dependence of the mass ratios $\frac{M_n}{M}$ on H is

$$M_n \sim 2M \left[\sin n\pi/6 + \frac{n\pi}{9 \ln h/Jh_0} \cos n\pi/6 \right], \quad (9)$$

where $h_0 = \sqrt{8\pi^3/e}$.

The Lagrangian (2) can be brought to standard Sine-Gordon form by performing the duality transformation $\theta \rightarrow \Phi$. The bosonized expressions of the spin operators change under this duality transformation as well. We find [9–11] $\vec{S}_n \rightarrow a_0 \vec{S}(x)$, $x = na_0$,

$$\begin{aligned} \vec{S}(x) &= \vec{J}(x) + (-1)^n \vec{n}(x), \\ J^z &= \frac{1}{\beta} \partial_x \Phi, \\ J^+ &= \frac{1}{2\pi a_0} \exp(-i\beta\Phi) \cos\left(\frac{2\pi}{\beta}\Theta - 2\delta x\right), \\ n^x(x) &= \frac{\Lambda}{\pi a_0} \cos(\beta\Phi(x)), \\ n^y(x) &= \frac{\Lambda}{\pi a_0} \sin(\beta\Phi(x)), \\ n^z(x) &= \frac{\Lambda}{\pi a_0} \cos\left(\frac{2\pi}{\beta}\Theta(x) - 2\delta x\right). \end{aligned} \quad (10)$$

Here Θ is the field dual to Φ , $n^a(x)$ are the components of the staggered magnetization, $J^{\pm,z}$ are the current operators, $na_0 = x$ and Λ is a nonuniversal coefficient. The quantity δ is the difference between the Fermi momenta for up spins and down spins. It is easily determined from the exact solution of the XXX Heisenberg chain in a magnetic field (see [4] and references therein) but is not important for the present work.

The dynamical magnetic susceptibilities for wavevectors close to the antiferromagnetic wave vector π ($\pi \pm 2\delta$ for the longitudinal part χ^{zz}) are then given by

$$\begin{aligned} \chi^{xx}(\omega, q) &\propto \int_{-\infty}^{\infty} dx \int_0^{\infty} dt e^{i(\omega+i\epsilon)t - i(q-\pi)x} \times \\ &\quad \times \langle [\cos \beta\Phi(t, x), \cos \beta\Phi(0, 0)] \rangle \\ \chi^{yy}(\omega, q) &\propto \int_{-\infty}^{\infty} dx \int_0^{\infty} dt e^{i(\omega+i\epsilon)t - i(q-\pi)x} \times \\ &\quad \times \langle [\sin \beta\Phi(t, x), \sin \beta\Phi(0, 0)] \rangle \\ \chi^{zz}(\omega, q) &\propto \int_{-\infty}^{\infty} dx \int_0^{\infty} dt e^{i(\omega+i\epsilon)t - i(q-\pi)x} \times \\ &\quad \times \langle [\cos\left(\frac{2\pi}{\beta}\Theta(t, x) - 2\delta x\right), \cos\left(\frac{2\pi}{\beta}\Theta(0, 0)\right)] \rangle. \end{aligned} \quad (11)$$

The transverse susceptibilities χ^{xx} and χ^{yy} can be determined exactly through the formfactor approach to quantum correlation functions [12–14] (our discussion follows [15]). The longitudinal susceptibility involves the dual field which is a nonlocal operator and cannot be treated in the same way. We therefore restrict our analysis to the transverse susceptibilities. As the longitudinal modes become soft at the incommensurate wavevectors $\pi \pm 2\delta$ rather than at the Neel wave vector π (where the transverse modes are soft) it is possible to separate χ^{zz} from $\chi^{\alpha\alpha}$, $\alpha = x, y$ experimentally by performing constant wavevector scans around $q = \pi \pm 2\delta$ and $q = \pi$ respectively.

Inserting a resolution of the identity in the correlation functions (11) we obtain formfactor expansions of the form

$$\chi^{xx}(\omega, q) = -2\pi \sum_{n=1}^{\infty} \sum_{\epsilon_i} \int \frac{d\theta_1 \dots d\theta_n}{(2\pi)^n n!} |F_{\epsilon_1 \dots \epsilon_n}^{\cos}(\theta_1 \dots \theta_n)|^2$$

$$\times \left\{ \frac{\delta[(\pi - q) - \sum_j M_j \sinh \theta_j]}{\omega - \sum_j M_j \cosh \theta_j + i\epsilon} - \frac{\delta[(\pi - q) + \sum_j M_j \sinh \theta_j]}{\omega + \sum_j M_j \cosh \theta_j + i\epsilon} \right\}, \quad (12)$$

and an analogous expansion for χ^{yy} . The quantities F^{cos} in (12) are the formfactors of the operator $\cos \beta \Phi$ and have been calculated exactly [12–14]. The expansion (12) is in terms of multiparticle states. In order to make contact with the neutron scattering experiments we are interested in the imaginary parts of the dynamical susceptibilities, which are proportional to the neutron scattering cross sections. Because all elementary excitations in the Sine Gordon theory have a gap, n -particle states will contribute to $\Im m \chi^{\alpha\alpha}(\omega, q)$ ($\alpha = x, y$) only at energies larger than the n -particle gap. In other words, by taking into account only the first few terms in the expansion (12) we obtain an exact expression for $\Im m \chi^{\alpha\alpha}(\omega, q)$ for energies below a threshold that depends on the omitted terms.

As the Sine-Gordon theory is Lorentz invariant the final answer for the susceptibilities cannot depend on ω and q independently but only on the combination

$$s = \sqrt{\omega^2 - (\pi - q)^2}. \quad (13)$$

The formfactor expansion is now readily performed using the results of [12–14] and the bootstrap procedure to determine breather formfactors. Using that $\cos \beta \Phi$ is even under charge conjugation [13,15] we find

$$\begin{aligned} \Im m \chi^{xx}(\omega, q) &\propto 2\pi \sum_{n=1}^{[1/\xi]} Z_{2n} \delta(s^2 - M_{2n}^2) \\ &+ \Re \frac{|F^{cos}[\theta(M_1, M_1, s)]_{11}|^2}{s\sqrt{s^2 - 4M_1^2}} \\ &+ 2\Re \frac{|F^{cos}[\theta(M, M, s)]_{+-}|^2}{s\sqrt{s^2 - 4M^2}} \\ &+ \dots \end{aligned} \quad (14)$$

where

$$\theta(m_1, m_2, s) = \text{arccosh} \left(\frac{s^2 - m_1^2 - m_2^2}{2m_1 m_2} \right). \quad (15)$$

Here the dependence of ξ on the applied field is given by (4) and Fig. 2. The first terms in (14) correspond to single-particle breather states. The (squares of the) breather formfactors are given by

$$\begin{aligned} Z_2 &= \frac{2(\sin 2\pi\xi)^2}{\cot \pi\xi} \\ &\times \exp \left[-2 \int_0^\infty \frac{dx}{x} \frac{(\sinh 2\xi x)^2 \sinh x(1-\xi)}{\cosh x \sinh 2x \sinh \xi x} \right], \\ Z_4 &= \frac{2(\sin 4\pi\xi)^2}{(\cot \pi\xi)^2 (\cot 3\pi\xi/2)^2} \\ &\times \exp \left[-2 \int_0^\infty \frac{dx}{x} \frac{(\sinh 4\xi x)^2 \sinh x(1-\xi)}{\cosh x \sinh 2x \sinh \xi x} \right]. \end{aligned} \quad (16)$$

The soliton-antisoliton formfactor is

$$\begin{aligned} |F_{+-}^{cos}(\theta)|^2 &= \frac{(2 \cot \pi\xi/2 \sinh \theta)^2}{\xi^2} \frac{\cosh \theta/\xi + \cos \pi/\xi}{\cosh 2\theta/\xi - \cos 2\pi/\xi} \\ &\times \exp \left[- \int_0^\infty \frac{dx}{x} \frac{[\cosh 2x \cos 2x\theta/\pi - 1] \sinh x(1-\xi)}{\cosh x \sinh 2x \sinh \xi x} \right], \end{aligned} \quad (17)$$

and the $B_1 B_1$ breather-breather formfactor is

$$\begin{aligned} |F_{11}^{cos}(\theta)|^2 &= \lambda^4 \frac{(\sinh \theta)^2}{(\sinh \theta)^2 + (\sin \pi\xi)^2} \\ &\times \exp \left[-8 \int_0^\infty \frac{dx}{x} \frac{\cos 2x\theta/\pi \sinh \xi x \sinh x \sinh x(1+\xi)}{(\sinh 2x)^2} \right], \end{aligned} \quad (18)$$

where

$$\lambda = 2 \cos \pi\xi/2 \sqrt{2 \sin \pi\xi/2} \exp \left[- \int_0^{\pi\xi} \frac{dx}{2\pi} \frac{x}{\sin x} \right]. \quad (19)$$

The next most important contribution (*i.e.* the term with the lowest threshold) in the expansion (14) comes from $B_1 B_3$ breather-breather states. It will contribute at energies larger than $M_1 + M_3$, where $M_{1,3}$ are given by (8).

In Fig. 3 we plot our result for $\chi^{xx}(\omega, q)$ as a function of $s/M = \sqrt{\omega^2 - (\pi - q)^2}/M$ (where M is given by (7)) for an applied field of $H = 3.5$ Tesla, which is one of the values studied experimentally in [1].

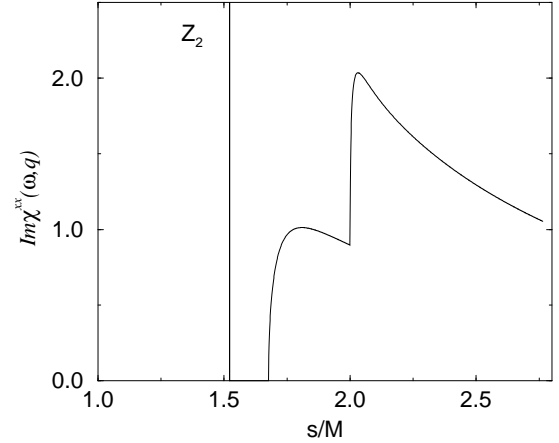


FIG. 3. Transverse susceptibility $\chi^{xx}(s)$ for $H = 3.5$ Tesla.

We see that there is one coherent mode at $s \approx 1.5M$ with weight $Z_2 \approx 1.02$. At $s \approx 1.68M$ the $B_1 B_1$ continuum appears and at $s = 2M$ the soliton-antisoliton continuum. The susceptibility is regular at both thresholds.

Fig. 4 shows $\chi^{xx}(\omega, q)$ as for $H = 7$ Tesla. The picture is qualitatively similar to the one at 3.5 Tesla although

the soliton-antisoliton threshold has become more pronounced. The weight of the delta-function corresponding to the breather B_2 has diminished to $Z_2'' \approx 0.97$. As the field increases a singularity develops at the $s = 2M$ threshold until at $H \approx 9.6$ Tesla the breather B_4 splits off the continuum. The situation at $H = 14$ Tesla is shown in Fig. 5. The weight of B_2 is $Z_2'' \approx 0.85$ whereas the fourth breather has only a very small spectral weight of $Z_4 \approx 0.01$.

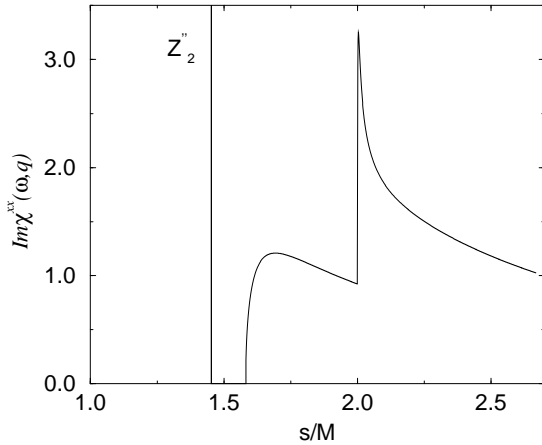


FIG. 4. Transverse susceptibility $\chi^{xx}(s)$ for $H = 7$ Tesla.

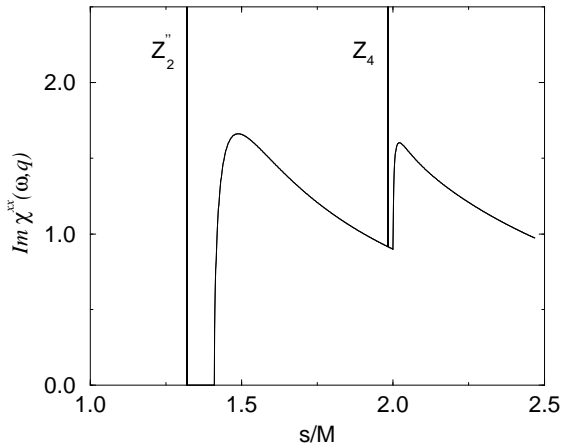


FIG. 5. Transverse susceptibility $\chi^{xx}(s)$ for $H = 14$ Tesla.

Let us now turn to $\Im m \chi^{yy}(\omega, q)$. It is clear from the form of the Hamiltonian (1) that this will be different from $\Im m \chi^{xx}(\omega, q)$. The formfactor expansion yields

$$\Im m \chi^{yy}(\omega, q) \propto 2\pi \sum_{n=1}^{[1/\xi]} Z_{2n-1} \delta(s^2 - M_{2n-1}^2)$$

$$\begin{aligned} & + 2\Re e \frac{|F^{sin}[\theta(M, M, s)]_{+-}|^2}{s\sqrt{s^2 - 4M^2}} \\ & + 2\Re e \frac{|F^{sin}[\theta(M_1, M_2, s)]_{12}|^2}{\sqrt{(s^2 - M_1^2 - M_2^2)^2 - 4M_1^2 M_2^2}} \\ & + \dots \end{aligned} \quad (20)$$

Here the breather formfactors are given by

$$\begin{aligned} Z_1 &= \frac{8(\cos \pi\xi/2)^4}{\cot \pi\xi/2} \\ &\times \exp \left[-2 \int_0^\infty \frac{dx}{x} \frac{\sinh \xi x \sinh x(1-\xi)}{\cosh x \sinh 2x} \right], \\ Z_3 &= \frac{4 \sin 3\pi\xi (\sin 3\pi\xi/2)^2}{(\cot \pi\xi)^2} \\ &\times \exp \left[-2 \int_0^\infty \frac{dx}{x} \frac{(\sinh 3\xi x)^2 \sinh x(1-\xi)}{\cosh x \sinh 2x \sinh \xi x} \right]. \end{aligned} \quad (21)$$

The soliton-antisoliton formfactor is found to be

$$\begin{aligned} |F_{+-}^{sin}(\theta)|^2 &= \frac{(2 \cot \pi\xi/2 \sinh \theta)^2}{\xi^2} \frac{\cosh \theta/\xi - \cos \pi/\xi}{\cosh 2\theta/\xi - \cos 2\pi/\xi} \\ &\times \exp \left[- \int_0^\infty \frac{dx}{x} \frac{[\cosh 2x \cos 2x\theta/\pi - 1] \sinh x(1-\xi)}{\cosh x \sinh 2x \sinh \xi x} \right]. \end{aligned} \quad (22)$$

Finally we take into account the $B_1 B_2$ breather-breather state which has a formfactor of

$$\begin{aligned} |F_{12}^{sin}(\theta)|^2 &= \frac{\tan \pi\xi}{2} |g(\theta - i\pi\xi/2)g(\theta + i\pi\xi/2)|^2 \lambda^6 \\ &\times \left(1 + \frac{1}{4 \cos \pi\xi/2 (\cosh \theta + \cos \pi\xi/2)} \right)^2 \\ &\times \exp \left[-8 \int_0^\infty \frac{dx}{x} \frac{\cos 2x\theta/\pi \sinh 2\xi x \sinh x \sinh x(1+\xi)}{(\sinh 2x)^2} \right] \\ &\times \exp \left[-8 \int_0^\infty \frac{dx}{x} \frac{\cosh 2x\xi \sinh \xi x \sinh x \sinh x(1+\xi)}{(\sinh 2x)^2} \right], \end{aligned} \quad (23)$$

where

$$g(x) = \frac{\sinh x}{\sinh x - i \sin \pi\xi}. \quad (24)$$

The next most important contribution to (20) is due to $B_1 B_1 B_1$ three breather states with a threshold at $3M_1$.

In Figs. 6-8 we plot $\chi^{yy}(s)$ for three different values of the applied field, namely $H = 3.5, 7, 14$ Tesla. The emerging picture remains qualitatively unchanged for all three values of H . There are two coherent modes corresponding to the breathers B_1 and B_3 . At $s = 2M$ the soliton-antisoliton continuum starts and at $s = M_1 + M_2$ we observe the onset of the $B_1 B_2$ breather-breather continuum. The latter one exhibits a singularity as a function of s . The weight of the delta functions corresponding to the breather B_1 decrease with increasing field:

$Z_1 \approx 2.07$, $Z'_1 \approx 2.04$ and $Z''_1 = 1.95$. For B_3 we find a decrease with increasing field after an initial increase: $Z_3 \approx 0.34$, $Z'_3 \approx 0.37$, $Z''_3 = 0.36$. Note that the spectral weight of the heavier B_3 particle is always significantly smaller.

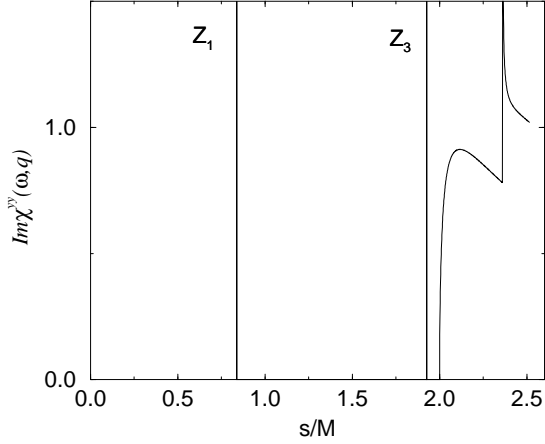


FIG. 6. Transverse susceptibility $\chi^{yy}(s)$ for $H = 3.5$ Tesla.

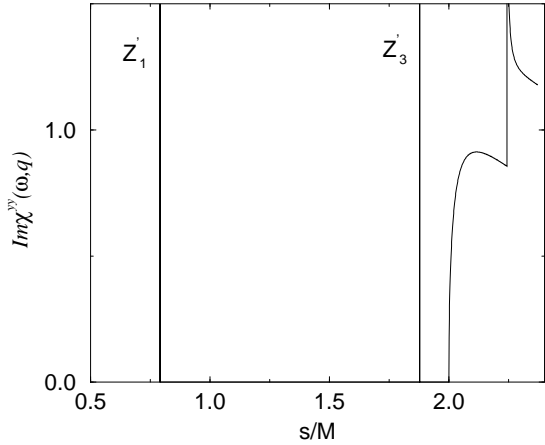


FIG. 7. Transverse susceptibility $\chi^{yy}(s)$ for $H = 7$ Tesla.

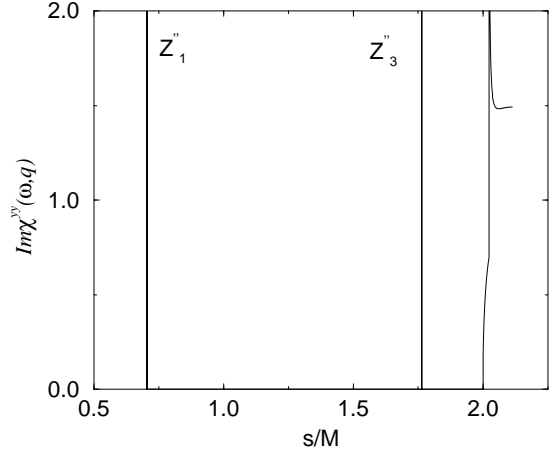


FIG. 8. Transverse susceptibility $\chi^{yy}(s)$ for $H = 14$ Tesla.

Let us now compare our results with the experimental findings. Our results for the imaginary part of the dynamical susceptibilities are consistent with the experiment at 7 Tesla (Fig. 1 (a) of [1]): as the beam was unpolarized the experiment observed $\frac{1}{2}(\chi^{xx} + \chi^{yy})$ (the contribution from χ^{zz} emerges only at energies greater than $g\mu_B H$). The observed peaks at 0.17meV, 0.34meV and 0.44meV correspond to the three breathers B_1 , B_2 and B_3 and agree very well with our prediction for the mass spectrum (8) and (7) (the first two peaks were already discussed in [3]). In order to compare our calculated weights of the delta-functions in the susceptibilities to the experimentally observed intensities one would need to convolve with the instrumental resolution. If we compare the maximal number of counts at the various peaks we find that the ratio in counts between the B_1 and B_2 peaks is approximately 3.7, which agrees well with the analytical result for $Z'_1 M_2 / Z'_2 M_1 \approx 3.85$. The B_3 peak sits on top of the $B_1 B_1$ continuum and from our analytical results we find that both contribute about the same amount to the total intensity. This means that about half of the counts found experimentally at 0.44meV are due to the B_3 breather, which agrees well with our results for $Z'_2 M_3 / Z'_3 M_2 \approx 3.35$.

Acknowledgements

We are grateful to G. Aeppli, C. Broholm, R. Coldea, R. Cowley, A. Millis and L.P. Regnault for important discussions. F.H.L.E. was supported by the EU under Human Capital and Mobility fellowship grant ERBCH-BGCT940709.

[1] D. C. Dender, P.R. Hammar, D.H. Reich, C. Broholm and G. Aeppli, preprint cond-mat/9704034.

- [2] M. Date *et.al.*, Suppl. Prog. Theor. Phys. **46** (1970) 194.
- [3] M. Oshikawa and I. Affleck, preprint `cond-mat/9706085`.
- [4] V. E. Korepin, A. G. Izergin, and N. M. Bogoliubov, *Quantum Inverse Scattering Method, Correlation Functions and Algebraic Bethe Ansatz* (Cambridge University Press, 1993).
- [5] V.E. Korepin and L.D. Faddeev, Theor. Mat. Phys. **25** (1975) 1039,
R. Dashen, B. Hasslacher and A. Neveu, Phys. Rev. **D11** (1975) 3424.
- [6] A.B. Zamolodchikov and Al.B. Zamolodchikov, Annals of Physics **120** (1979) 253.
- [7] H. Bergknoff and H. Thacker, Phys. Rev. **D19** (1979) 3666,
V.E. Korepin, Theor. Mat. Phys. **41** (1979) 169.
- [8] A. Luther, Phys. Rev. **B14** (1976) 2153.
- [9] I. Affleck, in *Fields, Strings and Critical Phenomena, Les Houches, Session XLIX*, edited by E. Brezin and J. Zinn-Justin (North-Holland, Amsterdam, 1988).
- [10] A.M. Tsvetik, *Quantum Field Theory in Condensed Matter Physics*, Cambridge University Press (1995).
- [11] I. Affleck, Nucl. Phys. **B265** (1986) 409,
F.D.M. Haldane, Phys. Rev. **B36** (1987) 5291,
D.G. Shelton, A.A. Nersesyan, A.M. Tsvetik, Phys. Rev. **B53** (1996) 8521.
- [12] M. Karowski and P. Weisz, Nucl. Phys. **B139** (1978) 455,
B. Berg, M. Karowski, P. Weisz, Phys. Rev. **D19** (1979) 2477.
- [13] F. A. Smirnov, *Form Factors in Completely Integrable Models of Quantum Field Theory*, World Scientific (1992).
- [14] S. Lukyanov, Comm. Math. Phys. **167** (1995) 183,
S. Lukyanov and A.B. Zamolodchikov, Nucl. Phys. **B493** (1997) 2541,
S. Lukyanov, preprint `hep-th/9703190`.
- [15] F.H.L. Eßler, A.M. Tsvetik and G. Delfino, preprint `cond-mat/9705196`, Phys. Rev. **B56**, November 1997.